

The Neuroscientist

<http://nro.sagepub.com>

Small-World Brain Networks

Danielle Smith Bassett and Ed Bullmore

Neuroscientist 2006; 12; 512

DOI: 10.1177/1073858406293182

The online version of this article can be found at:
<http://nro.sagepub.com/cgi/content/abstract/12/6/512>

Published by:

 SAGE Publications

<http://www.sagepublications.com>

Additional services and information for *The Neuroscientist* can be found at:

Email Alerts: <http://nro.sagepub.com/cgi/alerts>

Subscriptions: <http://nro.sagepub.com/subscriptions>

Reprints: <http://www.sagepub.com/journalsReprints.nav>

Permissions: <http://www.sagepub.com/journalsPermissions.nav>

Citations (this article cites 62 articles hosted on the SAGE Journals Online and HighWire Press platforms):
<http://nro.sagepub.com/cgi/content/refs/12/6/512>

Small-World Brain Networks

DANIELLE SMITH BASSETT and ED BULLMORE

Many complex networks have a small-world topology characterized by dense local clustering or cliquishness of connections between neighboring nodes yet a short path length between any (distant) pair of nodes due to the existence of relatively few long-range connections. This is an attractive model for the organization of brain anatomical and functional networks because a small-world topology can support both segregated/specialized and distributed/integrated information processing. Moreover, small-world networks are economical, tending to minimize wiring costs while supporting high dynamical complexity. The authors introduce some of the key mathematical concepts in graph theory required for small-world analysis and review how these methods have been applied to quantification of cortical connectivity matrices derived from anatomical tract-tracing studies in the macaque monkey and the cat. The evolution of small-world networks is discussed in terms of a selection pressure to deliver cost-effective information-processing systems. The authors illustrate how these techniques and concepts are increasingly being applied to the analysis of human brain functional networks derived from electroencephalography/magnetoencephalography and fMRI experiments. Finally, the authors consider the relevance of small-world models for understanding the emergence of complex behaviors and the resilience of brain systems to pathological attack by disease or aberrant development. They conclude that small-world models provide a powerful and versatile approach to understanding the structure and function of human brain systems. *NEUROSCIENTIST* 12(6):512–523, 2006. DOI: 10.1177/1073858406293182

KEY WORDS *Small-world network, Graph theory, Human brain functional networks, Functional magnetic resonance imaging*

What Is a Small-World Network?

The basic idea of a small-world network is immediately familiar to many of us from personal experience. We each have a social network of friends, relatives, and acquaintances. Our close friends and relatives are likely to constitute a cluster or clique of social contacts; for example, two of my close friends are likely to be friends with each other as well as with me. However, we may also have had the apparently surprising experience of traveling in a distant country or working in a strange city and discovering that some of the new people we meet in such a remote location are socially connected to people we already knew (friends of friends). It appears that social networks, as well as being locally clustered or cliquish, are remarkably extensive: The number of personal friendships mediating a social connection between

any two people can be surprisingly small given the size and geographical dispersion of the global population.

These qualitatively familiar concepts were translated to a more quantitative physical basis in an influential article by Watts and Strogatz (1998; Fig. 1). They constructed a simple computer model of a regular network or lattice, in which each node of the network was connected by a line or edge to each of its four nearest neighbors. This network structure or topology is highly clustered or cliquish by design, but to get from one node to another node on the opposite side of the lattice, one must traverse a large number of short-range connections. In other words, although the path length (or number of mediating edges) between neighboring nodes is short, the path length between distant nodes is long, and so the minimum path length averaged over all possible pairs of nodes in the network is also long. Watts and Strogatz investigated the change in network topology (measured in terms of local clustering and minimum path length) that resulted from randomly rewiring some of the lattice edges to create long-range connections between distant nodes. If many lattice edges were randomly rewired, the network naturally assumed the topological characteristics of a random graph (short path length and low clustering). But importantly, they found that the existence of even a few long-range connections greatly reduced the minimum path length of the network without affecting its local clustering to the same extent. Thus, they defined algorithmically for the first time a class of networks with topological properties similar to social networks, demonstrating both the high clustering of a lattice and the short path length of a random graph, which they called small-world networks.

From the Brain Mapping Unit, University of Cambridge, Department of Psychiatry, Addenbrooke's Hospital, Cambridge, United Kingdom (DSB, EB); Biological and Soft Systems, University of Cambridge, Department of Physics, Cavendish Laboratory, Cambridge, United Kingdom (DSB); and the Unit for Systems Neuroscience in Psychiatry, Genes, Cognition and Psychosis Program, National Institute of Mental Health, National Institutes of Health, Bethesda, Maryland (DSB).

DSB was supported by the Winston Churchill Foundation and the National Institutes of Health Graduate Partnerships Program. This work was also supported by a Human Brain Project grant from the National Institute of Biomedical Imaging & Bioengineering and the National Institute of Mental Health.

Address correspondence to: Ed Bullmore, Brain Mapping Unit, University of Cambridge, Department of Psychiatry, Addenbrooke's Hospital, Cambridge CB2 2QQ, UK (e-mail: etb23@cam.ac.uk).

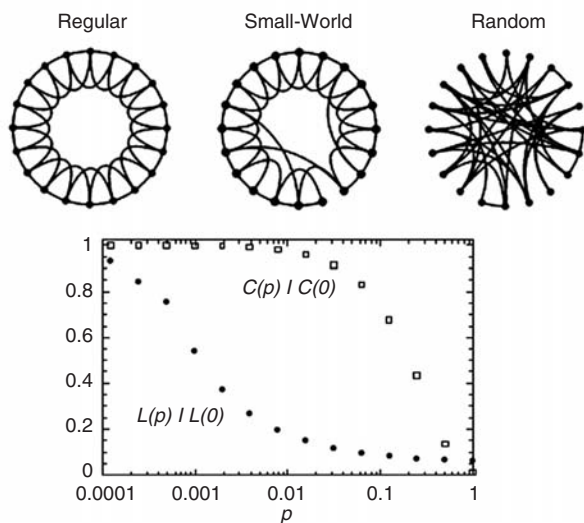


Fig. 1. Small-world diagram (Watts and Strogatz 1998). The computational model of small-world networks proposed by Watts and Strogatz (1998) began by connecting nodes with their nearest neighbors, producing a regular graph that had a high clustering coefficient and a high average path length. With a probability P , edges were then randomly rewired. When P was equal to unity, all edges were randomly rewired, and thus the network was perfectly random, having a short average path length and clustering coefficient. However, when P was between 0 and 1, there existed some dense local clustering, characteristic of regular networks, and some long-range connections, characteristic of random networks (i.e., the resultant graph was a small-world network with high clustering and low path length). Reprinted by permission from Macmillan Publishers Ltd: *Nature* 1998;393:440–2. Copyright 1998.

In the 8 years since small-world networks were described quantitatively in this way, there has been a remarkable profusion of studies seeking to clarify their mathematical properties and/or to explore their suitability as models of real-life networks. For example, the distinctive combination of high clustering and short path length has been reported in social networks of professionally collaborating actors or scientists; in infrastructural networks such as the Internet, power supply grids, or transport systems; and in biochemical systems such as cellular networks of protein-protein or gene-gene interactions. Small-world topology has been demonstrated empirically in complex networks at physical scales ranging from molecular to macroeconomic and in scientific contexts as diverse as ecology, computing, and linguistics (for a thorough review, see Boccaletti and others 2006).

Why Should We Think about the Brain as a Small-World Network?

There are empirical and theoretical reasons a priori why small worlds present an attractive model for brain network connectivity. Later, we will review the mathematical methodology and empirical findings in more detail; first, we briefly rehearse the main theoretical motivations.

1. The brain is a complex network on multiple spatial and time scales. This fact alone might motivate a small-world analysis of brain networks given the widespread occurrence of small-world properties in so many other complex networks and over a wide range of physical scales.
2. The brain supports both segregated and distributed information processing. Network architecture is regarded as a key substrate for sensorimotor and cognitive processing, which may be localized discretely in specialized regions or represented by coherent oscillations in large-scale distributed systems. Small-world topology comprises both high clustering (compatible with segregated or modular processing) and short path length (compatible with distributed or integrated processing).
3. The brain likely evolved to maximize efficiency and/or minimize the costs of information processing. Small-world topology is associated with high global and local efficiency of parallel information processing, sparse connectivity between nodes, and low wiring costs. Small-world networks can operate dynamically in a critical state, facilitating rapid adaptive reconfiguration of neuronal assemblies in support of changing cognitive states.

Mathematical Concepts

Complex systems can be better understood when we describe them mathematically as graphs. For graph analysis, the N individual components or agents comprising the system are called nodes and the K relations or connections between them are called edges (Fig. 2).

The edges of a graph can be directed or undirected: An undirected graph simply summarizes symmetric relations (such as correlations) between nodes, whereas a directed graph additionally models the causal relationships between nodes. Edges can also be categorized as weighted or unweighted: In an unweighted graph, all the edges are assumed to indicate relations of equivalent strength between nodes, whereas a weighted graph can be used to differentiate stronger and weaker connections.

Each node of a graph can be described in terms of the number of edges that connect to it: This is called the degree of a node, k . The nearest neighbors of a node are directly connected to it by a single edge. In a directed graph, we can distinguish between the in-degree (number of afferent edges) and the out-degree (number of efferent edges) of a node. The degree distribution of a graph is the probability distribution of k . Random graphs have an exponential degree distribution: $P(k) \sim e^{-\alpha k}$ (Albert and Barabási 2002). Several complex systems, such as the Internet and World Wide Web (WWW), have been found to have a power law distribution of the form $P(k) \sim k^{-\alpha}$, which implies a greater probability that nodes with a very large degree will exist in the graph (Albert and Barabási 2002). Thus, the power law degree distribution of the WWW is compatible with the existence of a few major hubs such as Google or Yahoo!, to which very many other sites are linked. Many physically embedded networks, such as transport or infrastructural

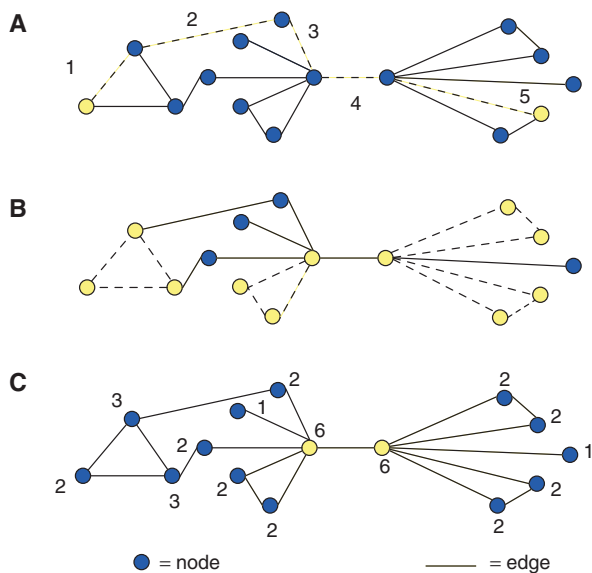


Fig. 2. Graph scheme: path length, clustering, average degree. Nodes are usually depicted by circular objects. Edges are the connections between these nodes. *A*, The path length between the two yellow nodes is defined as the fewest number of edges that must be traversed to get from one to the other. In this case, five edges must be followed, and therefore the path length between these two nodes is five. *B*, A high clustering coefficient means that if two nodes are both connected to a third node, then they are probably also connected to each other. The calculation of the clustering coefficient takes into account the number of connected triangles (shown here with yellow nodes and dashed edges). *C*, The degree of a node is equal to the number of edges connected to it. A hub is defined as a node that has a degree larger than the average degree. The average degree in this network is 3.3, and therefore, both nodes with degree 6 are hubs (shown in yellow).

systems, have an exponentially truncated power law distribution of the form $P(k) \sim k^{\alpha-1} e^{-k/k_c}$, which implies that the probability of highly connected hubs will be greater than in a random graph but smaller than in a scale-free network with a power law degree distribution (Amaral and others 2000).

The two key metrics of small worldness introduced by Watts and Strogatz (1998) are the clustering coefficient C and the minimum path length L . The path length between any two nodes is simply defined as the minimal number of edges that must be traversed to form a direct connection between the two nodes of interest (Watts and Strogatz 1998; Fig. 2). The clustering coefficient of a node is a measure of the number of edges that exist between its nearest neighbors (Schank and Wagner 2005); if all the nearest neighbors of an index node are also nearest neighbors of each other, then C will have its maximum normalized value (1). The minimum path length and clustering coefficient of the whole graph are estimated simply by averaging L_i and C_i for each of the $i = 1, 2, 3, \dots, N$ nodes it comprises. To evaluate the properties of a real-life network, these parameters must be compared to the mean

clustering coefficient and path length estimated in a random graph with the same number of nodes, edges, and degree distribution as the network of interest. In a random graph, the average minimum path length is typically short, $L_{\text{rand}} \sim \ln N / \ln([K/N] - 1)$, and the average clustering coefficient is typically small, $C_{\text{rand}} \sim (K/N)/N$ (Albert and Barabási 2002). For a small-world network, by definition, we expect the ratio $\lambda = L/L_{\text{rand}}$ to be approximately 1 and the ratio $\gamma = C/C_{\text{rand}}$ to be greater than 1. Therefore, a simple scalar measure of small worldness can be defined as $\sigma = \gamma/\lambda$, which will be greater than 1 if the network has the characteristic property of greater-than-random clustering and near-random path length (Humphries and others 2006).

More recent methodological work has developed alternative metrics of complex networks that can be related to C and L and may have some technical or conceptual advantages. For example, we can define the global efficiency of information transmission by a network as inversely proportional to the average minimum path length, $E_{\text{glob}} \sim 1/L$ (Latora and Marchiori 2001). Unlike path length, global efficiency can be measured in networks that are not composed of a single, large group of interconnected nodes. Global efficiency may also be preferable to path length as a metric of brain network topology because it is more immediately related to the functional efficiency of the system for information transmission between any two nodes via multiple parallel paths. This is attractive, compared to the more serial metric of path length, because the brain is known to instantiate parallel processing. We can also define the local efficiency or fault tolerance of a network as proportional to the clustering coefficient, $E_{\text{loc}} \sim C$. Both these efficiency measures can be compared to the maximum global and local efficiency of an ideal network, in which all possible connections between nodes are present and thus normalized to the range $0 < (E_{\text{glob}}, E_{\text{loc}}) < 1$.

Another potentially important metric for brain network analysis is some measure of cost. One simple cost function is the sum of edges between regions in the graph (Latora and Marchiori 2003); a costly network will have many edges. Many small-world networks in biology and sociology have been shown to have the economic property of delivering high global and local efficiency at relatively low cost (Latora and Marchiori 2003).

Several recent reviews provide a more extensive consideration of the mathematical basis of graph analysis of small-world networks (Albert and Barabási 2002; Costa and others 2006). There are also a number of generally accessible books describing the existence and characteristics of small-world networks in common experience (Buchanan 2003; Watts 2004a, 2004b).

Brain Anatomical Networks

The first graphical analyses of mammalian cortical networks, in the early 1990s, preceded the mathematical development of the small-world model but identified many features of anatomical connectivity that would later be recognized as compatible with it.

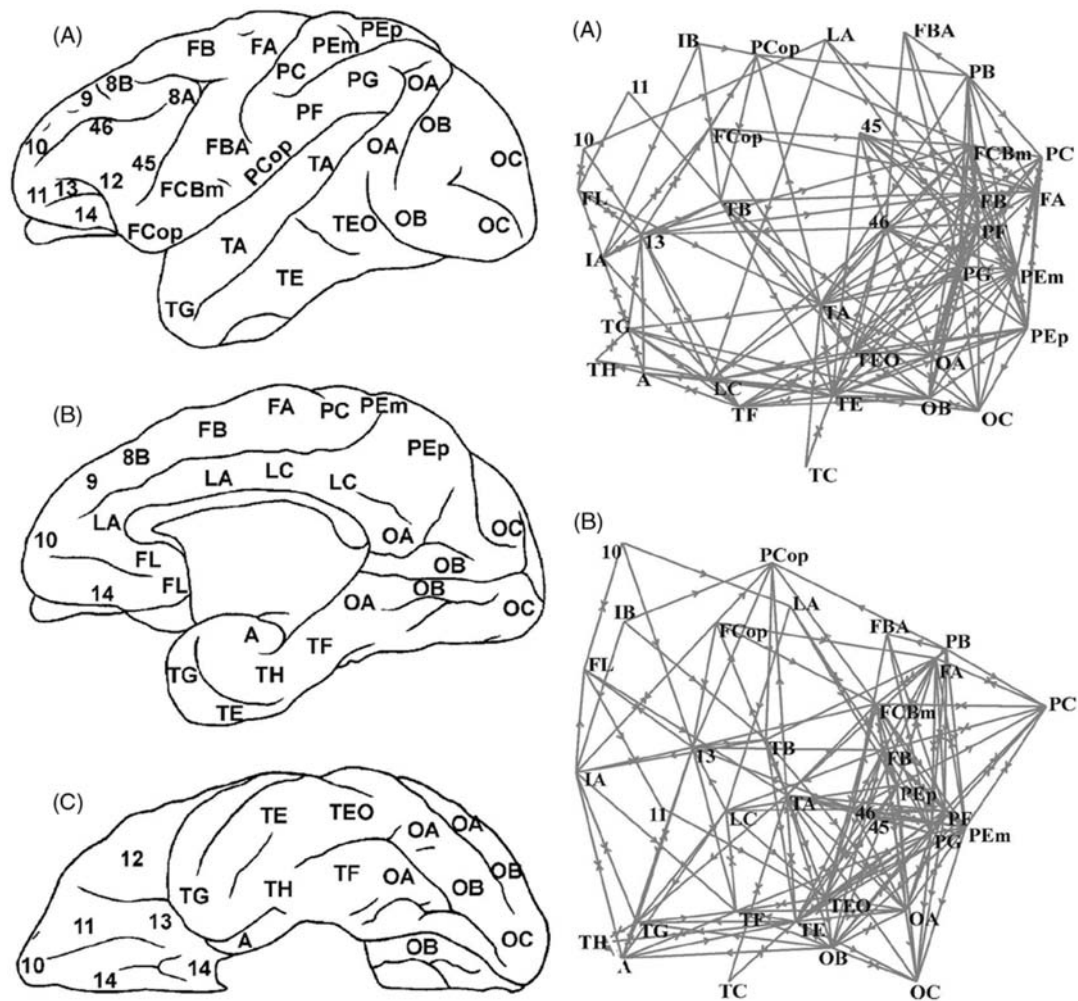


Fig. 3. Cortical connectivity maps (Stephan and others 2000). *Left*, A schematic map of the parcellation scheme of the macaque cortex used in Stephan and others (2000), showing the lateral aspect (A), medial aspect (B), and ventral aspect (C). *Right*, Graphical depictions of the functional connectivity in the macaque cortex constructed using nonmetric multidimensional scaling, a method that places nodes in close proximity if the connection between them is strong and places nodes far apart if the connection between them is weak. Data fit to distances (A) and data fit to square distances (B) show high clustering mostly between PC, PB, FA, FCBm, FB, PEP, PF, PEm, PG, TE, TEO, and OB (frontal and parietal regions). Sparse connections arise between, for example, IA, FL, IB, TH, and 11, suggesting small-world topology. Reprinted from *Philos Trans Roy Soc Lond B Biol Sci*, 355, Stephan KE, Hilgetag CC, O'Neill MA, Young MP, Kotter R, Computational analysis of functional connectivity between areas of primate cortex, 111-126, 2000, with permission from the Royal Society, London.

Felleman and Van Essen compiled an anatomical connectivity matrix from the prior tract-tracing literature that summarized 305 axonal connections between 32 areas of the visual cortex in the macaque monkey (Felleman and Van Essen 1991). Most connections were shown to be reciprocal (242 of the total), and the overall connection density (0.31) was somewhat sparse. Differentiation of these connections with respect to the laminar structure of the cortex was used to produce a hierarchy of 10 levels of cortical processing, which showed multiple segregated parallel processing streams with fewer connections between streams. Segregation of the ventral and dorsal streams was confirmed (Young and others 1995), whereas hierarchical graphical measures showed that the ventral

cluster was more clearly segregated than the dorsal cluster, whose nodes maintained more efferent edges (Hilgetag and others 2000; Costa and Sporns 2005).

Young and colleagues likewise considered anatomical connectivity matrices drawn from tract-tracing studies of the macaque monkey and the cat (Fig. 3; Young 1992, 1993). The connectivity matrix for the macaque visual cortex comprised 301 connections between 30 areas in the primate visual cortex, and connections were numerically coded as 0 (weak or absent) through 2 (strong and reciprocal). The topology of these connections was visualized using a multivariate technique called nonmetric multidimensional scaling (NMDS), which plots strongly connected areas in close proximity while maximizing the

Table 1. Global Topological Parameters for Small-World Networks in Anatomical Connectivity Matrices

Data	L	C	λ	γ	E_{glob}	E_{loc}	Cost
Macaque visual cortex	1.73	0.53	1.04	1.47	—	—	—
Macaque whole cortex	2.38	0.46	1.17	3.06	0.52	0.70	0.18
Cat cortex	1.81	0.55	1.06	1.77	0.69	0.83	0.38

Macaque visual cortex and whole cortex data are similar to those introduced by Felleman and Van Essen (1991) and Young (1993); cat cortex data are similar to those introduced by Scannell and others (1999). Classical small-world parameters, path length L and clustering C (λ and γ after scaling by random network parameters) are as summarized by Sporns and Zwi (2004). Economic small-world parameters, global and local efficiency (E_{glob} and E_{loc}), and cost are as reported by Latora and Marchiori (2003).

graphical distance between nonconnected areas. Thus, the resulting graph demonstrated strong interconnectivity of cortical areas comprising dorsal and ventral clusters with relatively few anatomical connections between these segregated processing streams. The results were summarized in terms of four organizing principles of the macaque visual cortex: 1) there are two segregated (dorsal and ventral) streams, 2) both streams are organized hierarchically, 3) the two streams converge in the same areas of the temporal and frontal association cortex, and 4) neighboring areas innervate each other strongly whereas distant areas are less likely to be connected, that is, networks are characterized by dense local clustering and a few long-range connections.

A similar approach was taken to the analysis of an anatomical connectivity matrix derived from tract-tracing studies in the cat. This matrix comprised a total of 1139 corticocortical connections between 65 cortical areas (average degree $k = 17.5$; Scannell and others 1995, 1999), which were numerically coded as either strong/dense (3), intermediate (2), or weak/sparse (1). The topology of the matrix was visualized using NMDS, and this showed four distinct clusters of strong local interconnectivity—designated visual, auditory, somatosensorimotor, and frontolimbic—with relatively sparse connectivity between clusters. The connectional topology was modeled by 1) nearest-neighbor and 2) next-door-but-one rules, both of which would generate regular or near-regular graphs. The nearest-neighbor and next-door-but-one models predicted, respectively, 26.1% and 56.6% of the real connections in the visual cluster, 27.9% and 61.6% in the auditory cluster, 18.2% and 44.4% in the somatosensorimotor cluster, and 20.2% and 50.2% in the frontolimbic cluster; globally, these two models predicted only 19.5% and 47.8% of the known anatomical connections. These results indicated that cortical connectivity was not well modeled as a regular graph (even within clusters or subgraphs).

Small-World Brain Anatomical Networks

The first nervous system to be formally quantified as a small-world network was at the microscopic scale of the neuronal network of *Caenorhabditis elegans*, which has been exactly described in terms of the 2462 synaptic connections between each of 282 constituent neurons. Using graph theoretical measures, the complete nervous system of *C. elegans* was shown to be neither random nor regular

but a small-world network, with an average path length of $L = 2.65$ and an average clustering coefficient of $C = 0.28$ (Watts and Strogatz 1998). Microscopic neuronal systems in the medial reticular formation of the vertebrate brain have also been shown to have small-world architecture (Humphries and others 2006).

In the study by Hilgetag and others (2000), the larger scale macaque and cat cortical connectivity matrices described above were formally shown to have small-world properties, that is, relatively high clustering ($\gamma \gg 1$) and short path lengths ($\lambda \sim 1$) compared to random networks (see Table 1). The same anatomical data have also been analyzed in terms of the economic small-world parameters—global and local efficiency and cost—and have high global efficiency and high local efficiency or fault tolerance at low cost (Latora and Marchiori 2003; see Table 1).

Why Do Brain Anatomical Networks Have Small-World Properties?

Given the strong empirical evidence that brain anatomical connectivity is sparse, locally clustered, and with a few long-range connections mediating short path lengths between any pair of regions, it is reasonable to ask why this small-world architecture has evolved.

We suppose that brain network architecture has likely evolved to maximize the complexity or adaptivity of function it can support while also minimizing costs. Below, we review some of the evidence that small-world topology is associated with low wiring costs and high dynamical complexity, suggesting that small-world brain network topology could indeed have been selected to optimize the economic problem of cost-effective information processing.

Wiring Costs and Small-World Brain Networks

Several aspects of brain structure are compatible with a selection pressure to minimize wiring costs: the segregation of white and gray matter, separation of visual cortical areas, scaling of the number of areas/neuronal density with brain size (Ringo 1991; Changizi 2001), organization of cortical areas and basal ganglia, existence of topographic maps, ocular dominance patterns, dimensions of axonal and dendritic arbors, and the fraction of gray matter occupied by axons and dendrites (Chklovskii and

others 2002; Stepanyants and others 2002; Chklovskii 2004). However, it is evident that the complete minimization of wiring would allow only local connections (Sik and others 1995) and not long-distance connections, leading to delayed information transfer and metabolic energy depletion (Allman 1998; Koch and Laurent 1999; Buzsáki and others 2004). To counteract this effect, the brain also minimizes energy costs by adding several long-distance connections, creating a small-world network (Karbowski 2001). The simultaneous minimization of wiring and energy costs may explain the cluster structure as well as long-range connectivity found throughout neural systems (Sik and others 1995; Hilgetag and Grant 2000; Sporns and others 2000; Buzsáki and others 2004; Zhigulin 2005).

Dynamical Complexity and Computational Small-World Networks

The dynamic consequences of a small-world brain anatomical network were first explicitly studied by Sporns and others in 2000. The interconnected regions of the macaque visual cortical network and cat cortical network were each separately injected with uncorrelated noise in a computational model that was allowed to run dynamically. After a period of time, the covariances of the dynamic processes between regional nodes were estimated (Sporns and others 2000, 2002) and thresholded to create an unweighted and undirected graph of computationally simulated network activity. The graphs showed high complexity, dense local clusters of connections, sparse interconnections between clusters, abundance of reciprocal connections and cycles, minimal wiring, and global and local efficiency (Vragovic and others 2005). Furthermore, it was shown that these graphs could easily match an input stimulus, produce a highly degenerate output stimulus, and allow both functional segregation and integration, all necessary for proper brain function (Sporns and others 2004). Sporns has corroborated this link between small-world topology and dynamical complexity by a different but complementary experimental approach (Sporns and others 2000). Instead of starting from an anatomical connectivity matrix with known small-world properties and simulating its complex dynamics, he has also started from a random graph and allowed its topology to evolve computationally to maximize the complexity of its dynamics. It turns out that computational graphs evolved for complexity have small-world topology (Fig. 4).

A strong relationship between small-world topology and dynamic complexity is confirmed by many other studies. Information propagates faster on many small-world networks of undirected uniformly coupled identical oscillators (Barahona and Pecora 2002; Hong and Choi 2002) with few exceptions (Atay and others 2006), allowing better computational power (Lago-Fernandez and others 2000) and increased stochastic resonance (Gao and others 2001), possibly due to its associated feedback system (Lu and others 2004). Synchronizability of these systems is found by computing the Laplacian spectrum (Barahona and Pecora 2002; Nishikawa and others 2003; Atay and

Biyikoglu 2005), and their robustness can be determined via edge removal (Lu and others 2004). Small-world topology has been associated with synchronizability $S \sim 0.1$, which marks a critical point in the dynamics of coupled oscillators, defining the transition from disordered to globally coherent oscillations as S becomes greater than 0.1. Pulse-coupled leaky integrate and fire oscillators show similar behavior (Masuda and Aihara 2004). Nonidentical Hodgkin-Huxley neurons coupled by excitatory synapses show fast responses in random networks, coherent oscillations in regular networks, and both fast responses and coherent oscillations in small-world networks (Lago-Fernandez and others 2000).

Brain Functional Networks

The first evidence for small-world properties of a brain functional network was provided by analysis of historical neuroanographic data, which identified a functional connection between regions of macaque cortex by the propagation of strychnine-induced epileptiform activity (Kötter and Sommer 2000; Stephan and others 2000). The functional network so defined had a short path length, $L = 2.17$, and high clustering, $C = 0.38$. However, most subsequent studies of brain functional networks have been based on human electroencephalography [EEG], magnetoencephalography [MEG], or functional MRI (fMRI).

From Functional Connectivity to Undirected Graph

For the anatomical and computational brain networks so far considered, it has been fairly straightforward to decide whether to draw an edge in the graph between any pair of regions or nodes. For the anatomical networks, we can refer to the literature on definitive tract-tracing studies to know if a certain axonal connection exists; for the computational networks, the exact topology is known by design. However, if we want to apply the same tools to analysis of brain functional networks, we will usually first have to derive an undirected graph from the data by applying a binary threshold to some continuous measure of association or functional connectivity (Friston 1994) between two neurophysiological time series recorded in distinct regional locations.

For instance, using EEG or fMRI, we can record a time series from each of several regions and then estimate the functional connectivity between a given pair of regional time series in terms of their mutual information, correlation, or partial correlation. We can also estimate functional connectivity in a restricted frequency range using coherence measures in the Fourier domain or correlations estimated in the wavelet domain (Fig. 5). However functional connectivity is estimated, the resulting matrix of pairwise associations will usually be binarized such that any association greater than threshold is represented as a line between the relevant regional nodes in a brain functional network (whereas any association less than threshold is represented as an absence of an edge between

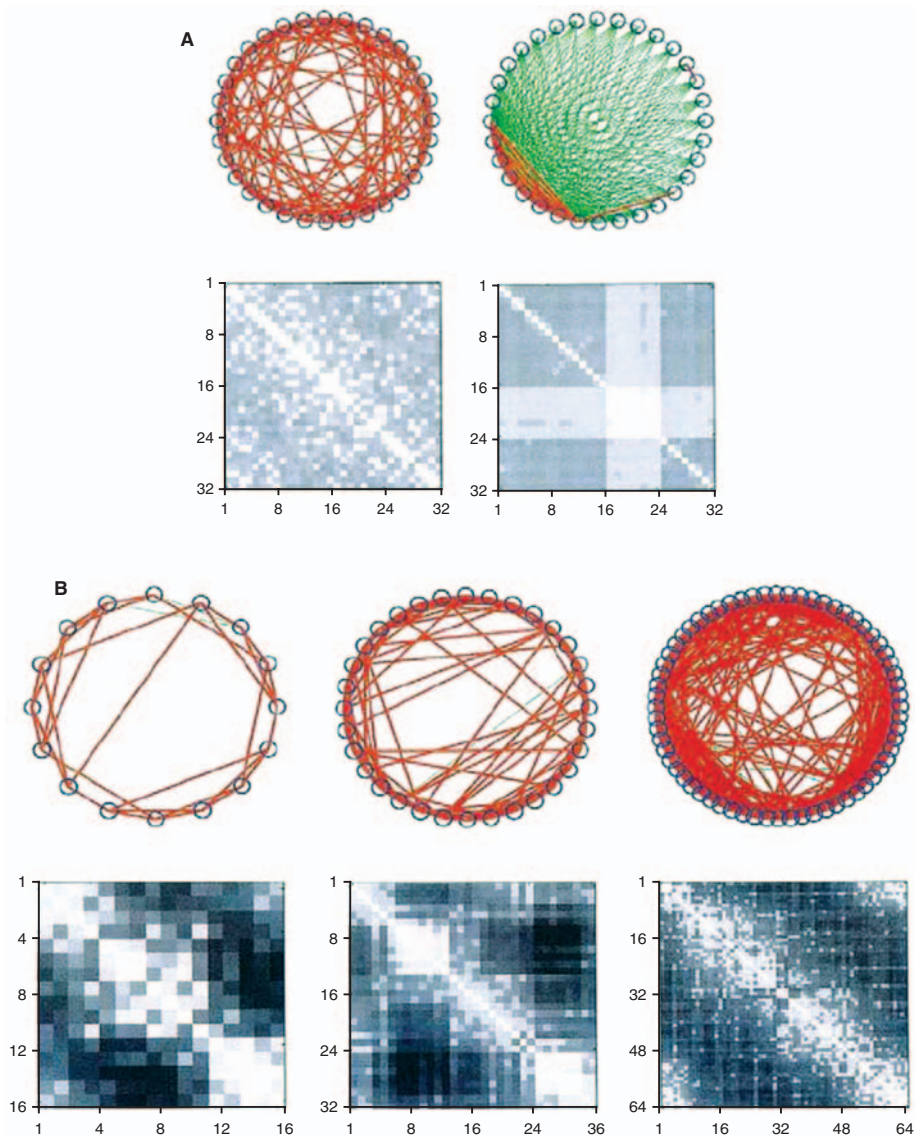


Fig. 4. Networks of high complexity (Sporns and others 2002). Types of graphs that represent high entropy, high integration, and high complexity along with the binary matrices used to create them (Sporns and others 2002). *A, Left*, A graph selected for high entropy in which nodes act fairly independently of each other. *Right*, A graph selected for high integration in which nodes are very dependent on each other for their dynamics. *B*, Three graphs ($N = 16$, $N = 32$, and $N = 64$) selected for high complexity in which nodes are both segregated and integrated simultaneously. The small-world properties of the macaque visual cortex are most like those emergent from a graph of high complexity. Parameters for the random, macaque visual cortex and high complexity graphs are respectively: average path lengths of 1.70, 1.77, 1.80 and clustering coefficients of 0.315, 0.554, 0.519 (Sporns and others 2000). Reprinted from Behav Brain Res, 20;135(1-2), Sporns O, Tononi G, Edelman GM, Theoretical neuroanatomy and the connectivity of the cerebral cortex, 69-74, 2002, with permission from Elsevier.

nodes). It follows that the reported topology of brain functional networks could depend considerably on the number of regions included, the chosen measure of association, and the thresholding rule (see Table 2 for a comparison). The relative merits of the various methodological options remain to be fully evaluated.

The first graph theoretical analysis of MEG data was reported by Stam (2004), who measured activity at 126 MEG sensors in five healthy individuals studied in a resting state with eyes closed. The pairwise association

between activity at different sensors was estimated using the synchronization likelihood, which is a measure of nonlinear as well as linear coupling between two time series, after the raw data had been filtered into classical EEG frequency bands (δ , θ , α , β , γ). The resulting functional connectivity matrices were thresholded (using a range of threshold values of the synchronization likelihood) to create a set of undirected graphs depicting brain functional networks specific to each of the frequency bands. It was reported that graphs from the α band (8–13 Hz) and

Table 2. Small-World Parameters for Functional Brain Networks in the Macaque and Healthy Human

Data	Connectivity Metric	<i>N</i>	<i>k</i>	<i>d</i>	<i>C</i>	<i>L</i>	λ	γ	σ
Macaque cortex (Stephan and others 2000)	Tract-tracing (binary)	39	6.1	0.15	0.38	2.17	1.01	2.46	2.44
Human MEG (Stam 2004)	Synchronization likelihood	126	15	0.12	~0.5	~5.0	~1.8	~4.2	~2.3
Human EEG (Micheloyannis and others 2006)	Synchronization likelihood	28	5	0.18	~0.4	~4.1	~1.0	~2.0	~2.0
Human fMRI (Eguíluz and others 2005)	Correlation	31,503	13.4	$4.3 \cdot 10^{-4}$	0.14	11.4	2.92	325	111
Human fMRI (Salvador, Suckling, Coleman, and others 2005)	Partial correlation	90	5.7	0.06	0.25	2.82	1.09	2.08	1.91
Human fMRI (Achard and others 2006)	Wavelet correlation	90	4.5	0.05	0.53	2.49	1.09	2.37	2.18

N = number of nodes; *k* = mean degree; *d* = connection density; *C* = clustering coefficient; *L* = path length; λ = path length scaled to random graph; γ = clustering coefficient scaled to random graph; σ = scalar small-worldness measure; MEG = magnetoencephalography; EEG = electroencephalography; fMRI = functional MRI. For those studies that did not provide these exact values in the text, ballpark values were taken from their figures and are preceded by a “~”, for example (Stam 2004; Micheloyannis and others 2006). Furthermore, two networks in Eguíluz and others (2005) could not be compared to random networks (because their *k* was smaller than $\ln(N)$) and therefore were not included.

β band (13–30 Hz) had regular, lattice-like topology whereas graphs from low- and high-frequency bands (δ , θ < 8 Hz or γ > 30 Hz) showed small-world properties.

A comparable study from the same group (Micheloyannis and others 2006) was based on EEG data recorded from 28 sensors in 14 subjects performing a working memory task. Functional connectivity was estimated using the synchronization likelihood, after the data had been filtered into classical frequency bands, then thresholded to create frequency-specific brain functional networks. However, in this case, there was evidence for small-world topology in all frequency bands. It is an interesting question to consider whether brain functional networks demonstrate small-world topology consistently across the full bandwidth of EEG/MEG signals or whether this topology is restricted to specific frequency intervals. The currently available data are inconclusive on this point.

Small-World Analyses of fMRI Data

Salvador and colleagues reported the first demonstration of small-world properties in brain functional networks derived from fMRI data. Functional MRI time series were recorded from five healthy volunteers in 90 cortical and subcortical regions during a no-task or resting state (Salvador, Suckling, Coleman, and others 2005; Salvador, Suckling, Schwarzbauer, and others 2005). Functional connectivity was estimated between each possible pair of time series using the partial correlation coefficient, and the connectivity matrix was probabilistically thresholded to create a sparse, undirected graph with $\lambda = 1.09$ and $\gamma = 2.08$. Multivariate analysis of the functional connectivity matrix,

using hierarchical cluster analysis and metric multidimensional scaling, demonstrated many of the same features previously described by multivariate analysis of anatomical connectivity matrices, including dense local connections between regions comprising visual, somatosensorimotor, and auditory-verbal clusters, and relatively sparse connectivity between functionally segregated dorsal and ventral components of the visual cortex.

The bandwidth of fMRI is narrow (approximately 0.01–1.0 Hz) compared to the physiological bandwidth of the brain and the instrumental bandwidth of EEG/MEG (approximately 0.01–100 Hz). This necessarily limits the extent to which fMRI can be used to investigate the frequency dependency of small-world brain functional networks. However, functional connectivity between fMRI time series can be estimated by coherence or partial coherence in the Fourier domain, which has demonstrated that long-range connections (e.g., between the frontal and parietal cortex) are stronger at frequencies less than 0.1 Hz (Salvador, Suckling, Schwarzbauer, and others 2005). An alternative mathematical approach is to decompose the fMRI time series into frequency bands using the wavelet transform (rather than the Fourier transform) and then estimate functional connectivity between regions in terms of the correlation between wavelet coefficients.

Wavelet-based functional connectivity analysis was introduced by Achard and colleagues who reported small-world properties of fMRI networks at all frequencies in the range from 0.007 to 0.45 Hz but most saliently in the frequency interval 0.03 to 0.06 Hz ($\lambda = 1.08$ and $\gamma = 2.38$; Figs. 5 and 6; Achard and others 2006). At a regional level of analysis, clustering was negatively correlated with the

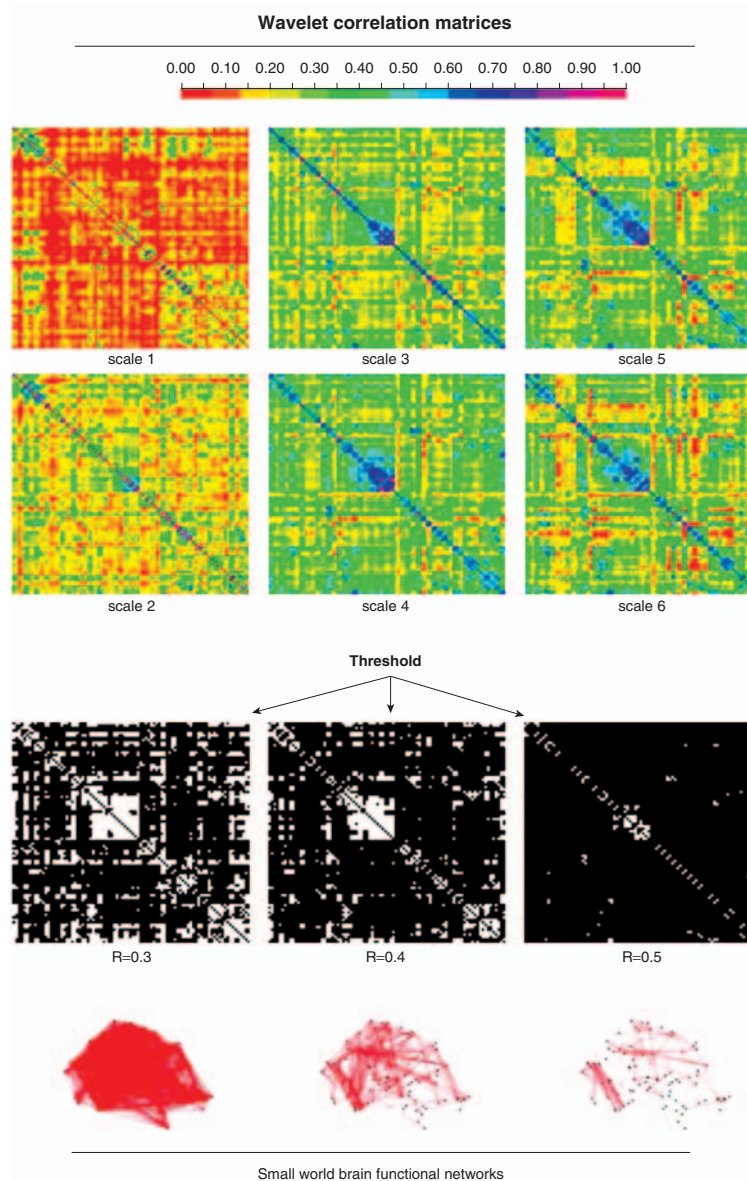


Fig. 5. Wavelet correlation matrices (Achard and others 2006). Method for defining brain graphs from functional MRI using a wavelet analysis to extract frequency-specific information. Scale 1 contains information about functional activity in the highest frequency range, 0.23 to 0.45 Hz, whereas scale 2 contains 0.11 to 0.23 Hz, scale 3 contains 0.06 to 0.11 Hz, scale 4 contains 0.03 to 0.06 Hz, scale 5 contains 0.01 to 0.03 Hz, and scale 6 contains 0.007 to 0.01 Hz. *Rows 1 and 2*, The average magnitude and distribution of correlations vary throughout the scale, with the highest average correlation being in scale 4 at 0.45 and the lowest average correlation in scale 1 at 0.12. *Row 3*, The correlation matrices are then thresholded to create binary matrices. *Row 4*, A high threshold creates a sparse matrix and a graph with few connections (*right*), whereas a low threshold creates a denser matrix and a graph with a high average degree; small-world features are most clearly visible at an intermediate threshold (*middle*). Reprinted from *J Neurosci*, 26(1), Achard S, Salvador R, Whitcher B, Suckling J, Bullmore E, A resilient, low-frequency, small-world human brain functional network with highly connected association cortical hubs, 63-72, 2006, with permission from the Society for Neuroscience.

physical distance of connections to a node: For example, areas of the unimodal association cortex had highly clustered, mostly short-range connections, whereas areas of the heteromodal association cortex had less clustered, more long-range connections. A similar observation has been made in analysis of anatomical connectivity matrices and proposed as a new way to classify cortical

areas as either highly specialized (locally clustered connections) or integrative (long-distance connections; Sporns and Zwi 2004).

The degree distribution of a complex network potentially provides an important clue to the processes constraining its formation and growth. For example, the power law degree distribution of the WWW is compatible

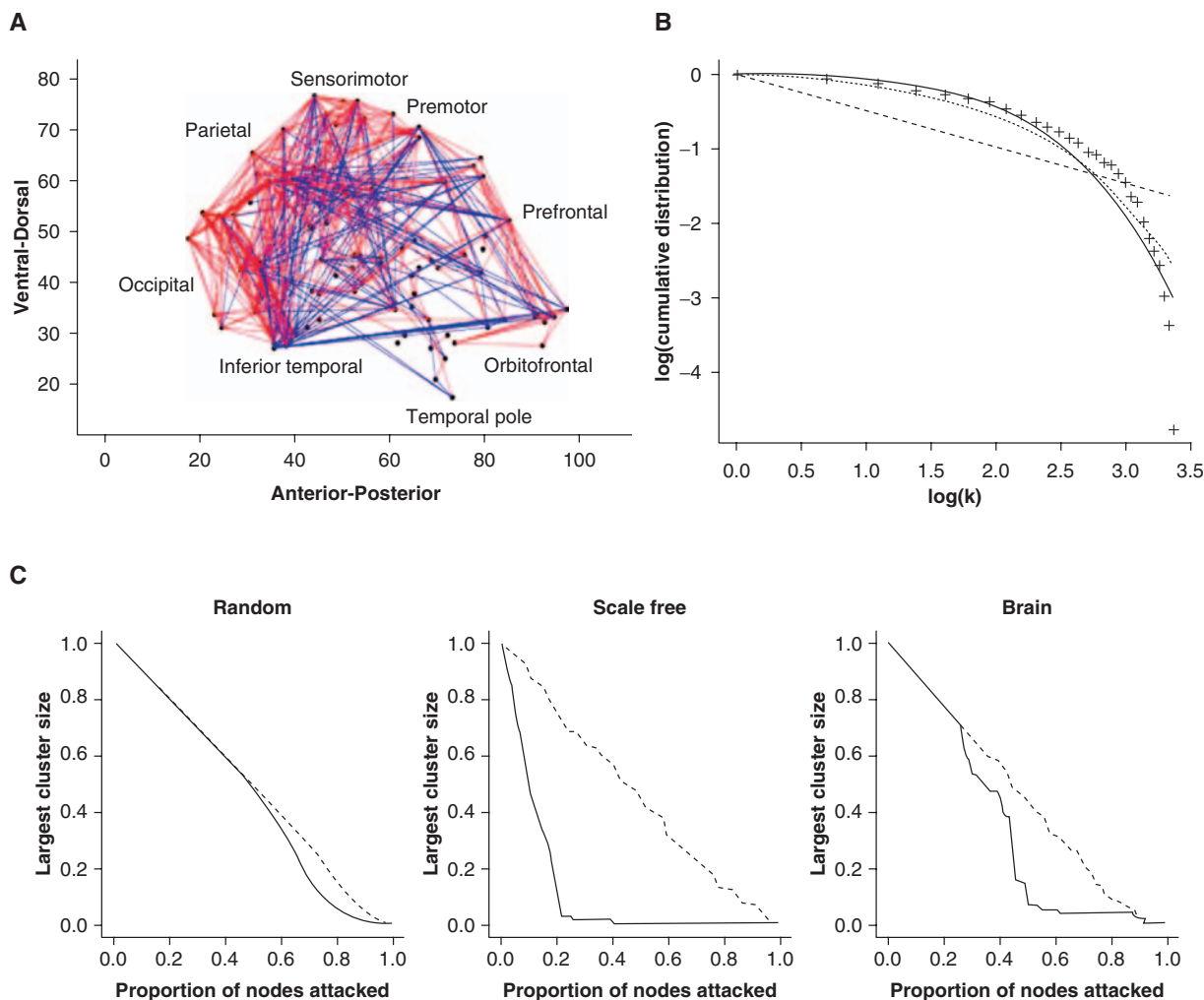


Fig. 6. Small-world functional brain networks (Achard and others 2006). Anatomical map of a small-world human brain functional network created by thresholding the scale 4 wavelet correlation matrix representing functional connectivity in the frequency interval 0.03 to 0.06 Hz. *A*, Four hundred five undirected edges, ~10% of the 4005 possible interregional connections, are shown in a sagittal view of the right side of the brain. Nodes are located according to the y and z coordinates of the regional centroids in Talairach space. Edges representing connections between nodes separated by a Euclidean distance <7.5 cm are red; edges representing connections between nodes separated by Euclidean distance >7.5 cm are blue. *B*, Degree distribution of a small-world brain functional network. Plot of the log of the cumulative probability of degree, $\log(P(k_i))$, versus log of degree, $\log(k_i)$. The plus sign indicates observed data, the solid line is the best-fitting exponentially truncated power law, the dotted line is an exponential, and the dashed line is a power law. *C*, Resilience of the human brain functional network (*right column*) compared with random (*left column*) and scale-free (*middle column*) networks. Size of the largest connected cluster in the network (scaled to maximum; y axis) versus the proportion of total nodes eliminated (x axis) by random error (dashed line) or targeted attack (solid line). The size of the largest connected cluster in the brain functional network is more resilient to targeted attack and about equally resilient to random error compared with the scale-free network. Reprinted from *J Neurosci*, 26(1), Achard S, Salvador R, Whitcher B, Suckling J, Bullmore E, A resilient, low-frequency, small-world human brain functional network with highly connected association cortical hubs, 63-72, 2006, with permission from the Society for Neuroscience.

with its growth by creation of new nodes, which preferentially form connections to existing hubs. One fMRI study has reported a power law degree distribution for a functional network of activated voxels (Eguíluz and others 2005). But the degree distribution of whole-brain fMRI networks of cortical regions has also been described as an exponentially truncated power law (Achard and others 2006), meaning broadly that the probability of very highly connected hubs is less in the brain than in the

WWW, but there is more probability of a hub in the brain than in a random graph. The hubs of this network were predominantly regions of the heteromodal and unimodal association cortex.

Truncated power law degree distributions are widespread in complex systems that are physically embedded or constrained, such as transport or infrastructural networks, and in systems in which nodes have a finite life span, such as the social network of collaborating Hollywood

movie stars. The existence of a truncated power law degree distribution in brain functional networks could likewise reflect the formative constraints of age of regions (Dorogovtsev and Mendes 2000), metabolic cost of maintaining long-range connections (Xulvi-Brunet and Sokolov 2002), or an upper limit on the number of connections that a single region can accommodate (Albert and Barabási 2000). More generally, it is known from computational studies that small-world networks can be created in a multitude of ways: by randomly rewiring links of a regular graph (Watts and Strogatz 1998), adding new links to it with a probability P (Newman and Watts 1999), or letting sites connect locally to geographically nearby sites (Ozik and others 2004). Plausible growth processes have also included spatial development (Kaiser and Hilgetag 2004a), accelerated growth (Krapivsky and others 2000), nodes provided with an initial attractiveness (Dorogovtsev and others 2000; Jeong and others 2003), growth constraints such as aging and cost (Amaral and others 2000; Dorogovtsev and Mendes 2000), competitive nodes (Bianconi and Barabási 2001), penalizing distance while adding volume and growth-direction constraints (Kaiser and Hilgetag 2004b), pruning (Humphries and others 2006), stochastic dynamics (Humphries and others 2006), and local addition, rewiring, or removal of nodes or edges (Albert and Barabási 2000). It will be interesting in the future to measure developmental changes in small-world brain networks as a way to better understand which of these possible growth rules are most important biologically.

Emergent Properties and Pathology of Small-World Networks

The topology of a brain network dictates not only its possible physical dynamics but also its emergent properties. For example, small-world networks have been shown to allow higher rates of information processing and learning than random graphs do (Simard and others 2005). This suggests that changes in cognitive state or cognitive capacity might be associated with (potentially rapid) changes in the configuration of brain functional networks. Currently, little is known about the cognitive correlates of normal variation in small-world parameters of fMRI or EEG/MEG networks, but Stam and colleagues (2006) have reported that cognitive decline due to Alzheimer disease is associated with increased path length (or reduced global efficiency) of EEG networks in the β band.

The functional resilience of brain networks to pathological attack can be modeled by deleting one or more nodes from the network and reestimating its small-world parameters. Deletion of any node might be expected to increase path length (reduce global efficiency), but deletion of hubs will have especially detrimental effects on overall network performance. Achard and colleagues (2006) measured path length of a brain functional network as it was degraded by random deletion of nodes and by targeted attack on the association cortical hubs. They found that the brain network was as resilient to random attack, and more resilient to targeted attack, than a comparable graph with a power law degree distribution (Fig. 6).

This suggests that the truncated power law degree distribution of brain networks, as well as possibly reflecting physical constraints on network growth, might also reflect a selection pressure favoring network topologies that are functionally resistant to local pathological attack. It is likewise plausible that this degree distribution might be important in limiting the synchronizability of the network to less than the critical threshold for globally coherent oscillations manifest clinically as epileptic seizures (Percha and others 2005).

Conclusion

Nervous systems are anatomically connected as small-world networks at macro and micro scales. This is a fit topological solution to the problem of economically delivering complex or adaptive network dynamics. In humans, there have been several recent reports of small-world brain functional networks measured using fMRI or MEG/EEG, but there is much still to learn about the (presumably small-world) topology of human brain anatomical networks; the relationships among graphical parameters of brain networks, their development, and emergent properties; and the impact of neuropsychiatric disorders and drugs on small-world brain networks.

References

- Achard S, Salvador R, Whitcher B, Suckling J, Bullmore E. 2006. A resilient, low-frequency, small-world human brain functional network with highly connected association cortical hubs. *J Neurosci* 26:63–72.
- Albert R, Barabási A-L. 2000. Topology of evolving networks: local events and universality. *Phys Rev Lett* 85:5234–7.
- Albert R, Barabási A-L. 2002. Statistical mechanics of complex networks. *Rev Mod Phys* 74(1):47.
- Allman JM. 1998. *Evolving brains*. New York: Scientific American.
- Amaral LAN, Scala A, Barthelemy M, Stanley HE. 2000. Classes of small-world networks. *Proc Natl Acad Sci U S A* 97:11149–52.
- Atay FM, Biyikoglu T. 2005. Graph operations and synchronization of complex networks. *Phys Rev E* 72:016217.
- Atay FM, Biyikoglu T, Jost J. 2006. Synchronization of networks with prescribed degree distributions. *IEEE Transactions on Circuits and Systems Part I: Regular Papers* 53(1):92–8.
- Barahona M, Pecora LM. 2002. Synchronization in small-world systems. *Phys Rev Lett* 89:054101.
- Bianconi G, Barabási A-L. 2001. Competition and multiscaling in evolving networks. *Europhys Lett* 54:436.
- Boccaletti S, Latora V, Moreno Y, Chavez M, Hwang DU. 2006. Complex networks: structure and dynamics. *Phys Rep* 424:175–308.
- Buchanan M. 2003. *Small world: uncovering nature's hidden networks*: London: Orion.
- Buzsáki G, Geisler C, Henze DA, Wang X-J. 2004. Interneuron diversity series: circuit complexity and axon wiring economy of cortical interneurons. *Trends Neurosci* 27:186–93.
- Changizi MA. 2001. Principles underlying mammalian neocortical scaling. *Biol Cybern* 84:207–15.
- Chklovskii DB. 2004. Synaptic connectivity and neuronal morphology: two sides of the same coin. *Neuron* 43:609–17.
- Chklovskii DB, Schikorski T, Stevens CF. 2002. Wiring optimization in cortical circuits. *Neuron* 34:341–7.
- Costa LdF, Rodrigues FA, Travieso G, Boas PRV. 2006. Characterization of complex networks: a survey of measurements. Available from: <http://arxiv.org/abs/cond-mat/0505185>.
- Costa LdF, Sporns O. 2005. Hierarchical features of large-scale cortical connectivity. *Eur Phys JB* 48:567–73.
- Dorogovtsev SN, Mendes JFF. 2000. Evolution of networks with aging of sites. *Phys Rev E* 62:1842.

- Dorogovtsev SN, Mendes JFF, Samukhin AN. 2000. Structure of growing networks with preferential linking. *Phys Rev Lett* 85:4633.
- Eguíluz VM, Chialvo DR, Cecchi GA, Baliki M, Apkarian AV. 2005. Scale-free brain functional networks. *Phys Rev Lett* 94:018102.
- Felleman DJ, Van Essen DC. 1991. Distributed hierarchical processing in the primate cerebral cortex. *Cereb Cortex* 1:1–47.
- Friston KJ. 1994. Functional and effective connectivity in neuroimaging: a synthesis. *Hum Brain Mapp* 2:56–78.
- Gao Z, Hu B, Hu G. 2001. Stochastic resonance of small-world networks. *Phys Rev E* 65:016209.
- Hilgetag CC, Burns GAPC, O'Neill MA, Scannell JW. 2000. Anatomical connectivity defines the organization of clusters of cortical areas in the macaque and the cat. *Philos Trans R Soc Lond B Biol Sci* 355:91.
- Hilgetag CC, Grant S. 2000. Uniformity, specificity and variability of corticocortical connectivity. *Philos Trans R Soc Lond B Biol Sci* 355:7–20.
- Hong H, Choi MY. 2002. Synchronization on small-world networks. *Phys Rev E* 65:026139.
- Humphries M, Gurney K, Prescott T. 2006. The brainstem reticular formation is a small-world, not scale-free, network. *Philos Trans R Soc Lond B Biol Sci* 273:503–11.
- Jeong H, Neda Z, Barabási A-L. 2003. Measuring preferential attachment for evolving networks. *Europhys Lett* 61:567–72.
- Kaiser M, Hilgetag CC. 2004a. Spatial growth of real-world networks. *Phys Rev E* 69:036103.
- Kaiser M, Hilgetag CC. 2004b. Modelling the development of cortical systems networks. *Neurocomputing* 2004:297–302.
- Karbowski J. 2001. Optimal wiring principle and plateaus in the degree of separation for cortical neurons. *Phys Rev Lett* 86:3674.
- Koch C, Laurent G. 1999. Complexity and the nervous system. *Science* 284:96–8.
- Kötter R, Sommer FT. 2000. Global relationship between structural connectivity propagation in the cerebral cortex. *Philos Trans R Soc Lond B Biol Sci* 355:127–34.
- Krapivsky PL, Redner S, Leyvraz F. 2000. Connectivity of growing random networks. *Phys Rev Lett* 85:4629.
- Lago-Fernandez LF, Huerta R, Corbacho F, Siguenza JA. 2000. Fast response and temporal coherent oscillations in small-world networks. *Phys Rev Lett* 84:2758–61.
- Latora V, Marchiori M. 2001. Efficient behavior of small-world networks. *Phys Rev Lett* 87:198701.
- Latora V, Marchiori M. 2003. Economic small-world behavior in weighted networks. *Euro Phys JB* 32:249–63.
- Lu J, Yu K, Chen G, Cheng D. 2004. Characterizing the synchronizability of small-world dynamical networks. *IEEE Transactions on Circuits and Systems Part I: Regular Papers* 51:787–96.
- Masuda N, Aihara K. 2004. Global and local synchrony of coupled neurons in small-world networks. *Biol Cybern* 90:302–9.
- Micheloyannis S, Pachou E, Stam CJ, Vourkas M, Erimaki S, Tsirka V. 2006. Using graph theoretical analysis of multi channel EEG to evaluate the neural efficiency hypothesis. *Neurosci Lett* 402:273–7.
- Newman MEJ, Watts DJ. 1999. Scaling and percolation in the small-world network model. *Phys Rev E* 60:7332.
- Nishikawa T, Motter AE, Lai Y-C, Hoppensteadt FC. 2003. Heterogeneity in oscillator networks: are smaller worlds easier to synchronize? *Phys Rev Lett* 91:014101.
- Ozik J, Hunt BR, Ott E. 2004. Growing networks with geographical attachment preference: emergence of small worlds. *Phys Rev E* 69:026108.
- Percha B, Dzakpasu R, Zochowski M, Parent J. 2005. Transition from local to global phase synchrony in small world neural network and its possible implications for epilepsy. *Phys Rev E* 72:031909.
- Ringo JL. 1991. Neuronal interconnection as a function of brain size. *Brain Behav Evol* 38:1–6.
- Salvador R, Suckling J, Coleman MR, Pickard JD, Menon D, Bullmore E. 2005. Neurophysiological architecture of functional magnetic resonance images of human brain. *Cereb Cortex* 15:1332–42.
- Salvador R, Suckling J, Schwarzbauer C, Bullmore E. 2005. Undirected graphs of frequency-dependent functional connectivity in whole brain networks. *Philos Trans R Soc Lond B Biol Sci* 360:937.
- Scannell JW, Blakemore C, Young MP. 1995. Analysis of connectivity in the cat cerebral cortex. *J Neurosci* 15:1463–83.
- Scannell JW, Burns GAPC, Hilgetag CC, O'Neill MA, Young MP. 1999. The connective organization of the cortico-thalamic system of the cat. *Cereb Cortex* 9:277–99.
- Schank T, Wagner D. 2005. Approximating clustering coefficient and transitivity. *Journal of Graph Algorithms and Applications* 9: 265–75.
- Sik A, Penttonen M, Ylinen A, Buzsáki G. 1995. Hippocampal CA1 interneurons: an in vivo intracellular labeling study. *J Neurosci* 15:6651–65.
- Simard D, Nadeau L, Kroger H. 2005. Fastest learning in small-world neural networks. *Phys Lett A* 336:8–15.
- Sporns O, Chialvo DR, Kaiser M, Hilgetag CC. 2004. Organization, development and function of complex brain networks. *Trends Cogn Sci* 8:418–25.
- Sporns O, Tononi G, Edelman GM. 2000. Theoretical neuroanatomy: relating anatomical and functional connectivity in graphs and cortical connection matrices. *Cereb Cortex* 10:127–41.
- Sporns O, Tononi G, Edelman GM. 2002. Theoretical neuroanatomy and the connectivity of the cerebral cortex. *Behav Brain Res* 135:69–744.
- Sporns O, Zwi J. 2004. The small world of the cerebral cortex. *Neuroinformatics* 2:145–62.
- Stam CJ. 2004. Functional connectivity patterns of human magnetoencephalographic recordings: a “small-world” network? *Neurosci Lett* 355:25–8.
- Stam CJ, Jones BF, Nolte G, Breakspear M, Scheltens P. 2006. Small-world networks and functional connectivity in Alzheimer's disease. *Cereb Cortex*. Epub ahead of print February 1, 2006.
- Stepanyants A, Hof PR, Chklovskii DB. 2002. Geometry and structural plasticity of synaptic connectivity. *Neuron* 34:275–88.
- Stephan K, Hilgetag CC, Burns GAPC, O'Neill MA, Young MP, Kötter R. 2000. Computational analysis of functional connectivity between areas of primate cerebral cortex. *Philos Trans R Soc Lond B Biol Sci* 355:111–26.
- Vragovic I, Louis E, Diaz-Guilera A. 2005. Efficiency of informational transfer in regular and complex networks. *Phys Rev E* 71:036122.
- Watts DJ. 2004a. Six degrees: the new science of networks. New York: Vintage.
- Watts DJ. 2004b. Small worlds: the dynamics of networks between order and randomness. Princeton (NJ): Princeton University Press.
- Watts DJ, Strogatz SH. 1998. Collective dynamics of “small-world” networks. *Nature* 393:440–2.
- Xulvi-Brunet R, Sokolov IM. 2002. Evolving networks with disadvantaged long-range connections. *Phys Rev E* 66:026118.
- Young MP. 1992. Objective analysis of the topological organization of the primate cortical visual system. *Nature* 358:152–5.
- Young MP. 1993. The organization of neural systems in the primate cerebral cortex. *Proc R Soc Lond B* 252:13–8.
- Young MP, Scannell JW, O'Neill MA, Hilgetag CC, Burns GAPC, Blakemore C. 1995. Non-metric multidimensional scaling in the analysis of neuroanatomical connection data and the organization of the primate cortical visual system. *Philos Trans R Soc Lond B Biol Sci* 348:281–308.
- Zhigulin VP. 2005. Dynamical motifs: building blocks of complex dynamics in sparsely connected random networks. *Phys Rev Lett* 92:238701.